Redox Biology 12 (2017) 864–871

Contents lists available at ScienceDirect

Redox Biology

journal homepage: www.elsevier.com/locate/redox

Research Paper

CNS bioavailability and radiation protection of normal hippocampal neurogenesis by a lipophilic Mn porphyrin-based superoxide dismutase mimic, MnTnBuOE-2-PyP^{5+}

David Leu[a,b], Ivan Spasojevic[c,d], Huy Nguyen[a], Brian Deng[a,b], Artak Tovmasyan[e], Tin Weitner[e], Romulo S. Sampaio[e], Ines Batinic-Haberle[e,*], Ting-Ting Huang[a,f,**]

[a] Department of Neurology and Neurological Sciences, Stanford University School of Medicine, Stanford, CA, USA
[b] Palo Alto Veterans Institute for Research, Palo Alto, CA, USA
[c] Duke Cancer Institute, Pharmaceutical Research Shared Resource, PK/PD Core laboratory, Duke University Medical Center, Durham, NC, USA
[d] Department of Medicine, Duke University Medical Center, Durham, NC, USA
[e] Department of Radiation Oncology, Duke University Medical Center, Durham, NC, USA
[f] Geriatric Research, Education, and Clinical Center, VA Palo Alto Health Care System, Palo Alto, CA, USA

ARTICLE INFO

Keywords:
Mn porphyrin
Bioavailability
BMX-001
Hippocampus
Neurogenesis
Radioprotection

ABSTRACT

Although radiation therapy can be effective against cancer, potential damage to normal tissues limits the amount that can be safely administered. In central nervous system (CNS), radiation damage to normal tissues is presented, in part, as suppressed hippocampal neurogenesis and impaired cognitive functions. Mn porphyrin (MnP)-based redox active drugs have demonstrated differential effects on cancer and normal tissues in experimental animals that lead to protection of normal tissues and radio- and chemo-sensitization of cancers. To test the efficacy of MnPs in CNS radioprotection, we first examined the tissue levels of three different MnPs – MnTE-2-PyP^{5+} (MnE), MnTnHex-2-PyP^{5+} (MnHex), and MnTnBuOE-2-PyP^{5+} (MnBuOE). Nanomolar concentrations of MnHex and MnBuOE were detected in various brain regions after daily subcutaneous administration, and MnBuOE was well tolerated at a daily dose of 3 mg/kg. Administration of MnBuOE for one week before cranial irradiation and continued for one week afterwards supported production and long-term survival of newborn neurons in the hippocampal dentate gyrus. MnP-driven *S*-glutathionylation in cortex and hippocampus showed differential responses to MnP administration and radiation in these two brain regions. A better understanding of how preserved hippocampal neurogenesis correlates with cognitive functions following cranial irradiation will be helpful in designing better MnP-based radioprotection strategies.

1. Introduction

One of the significant challenges in radiation therapy of brain cancers is its negative impact on normal brain functions, which often limits the level of radiation that can be safely administered. Radiation therapy to the central nervous system (CNS) results in neurocognitive defects commonly recognized as the late effects of radiation therapy [1,2]. In experimental animals, cranial irradiation causes persistent oxidative stress and neuroinflammation [3–5] and a subsequent reduction in hippocampal neurogenesis and attrition of dendritic structures [6–9]. Antioxidant enzymes, including the extracellular superoxide dismutase (EC-SOD) and the mitochondrially targeted catalase, used within the context of transgenic animals have shown promising radiation protection of normal cognitive functions via preservation of hippocampal neurogenesis and dendritic structures [8,10]. The data suggested that antioxidant supplements may be beneficial for normal tissue protection against radiation damage in the CNS.

To translate the basic research findings into clinical practice, the genetic approach needs to be replaced with pharmacological agents for ease of administration. The Mn porphyrin (MnP)-based redox active drugs are developed based on structure-activity relationship for their actions as SOD mimics [11]. The biologically compatible reduction potential of MnPs allows them to oxidize and reduce superoxide equally well, thus functioning as both anti- and pro-oxidants. A large body of studies over the years suggests that MnPs can also undergo diverse interactions with other reactive species, such as reducing peroxynitrite,

* Correspondence to: Department of Radiation Oncology, Duke University Medical Center, 281b MSRB I, Research Drive, Durham, NC 27710, USA.
** Correspondence to: Department of Neurology and Neurological Sciences, Stanford University School of Medicine, Geriatric Research, Education, and Clinical Center, VA Palo Alto Health Care System, 3801 Miranda Avenue, Building 100, D3-101, Palo Alto, CA 94304, USA.

http://dx.doi.org/10.1016/j.redox.2017.04.027
Received 28 January 2017; Received in revised form 12 April 2017; Accepted 13 April 2017
Available online 22 April 2017

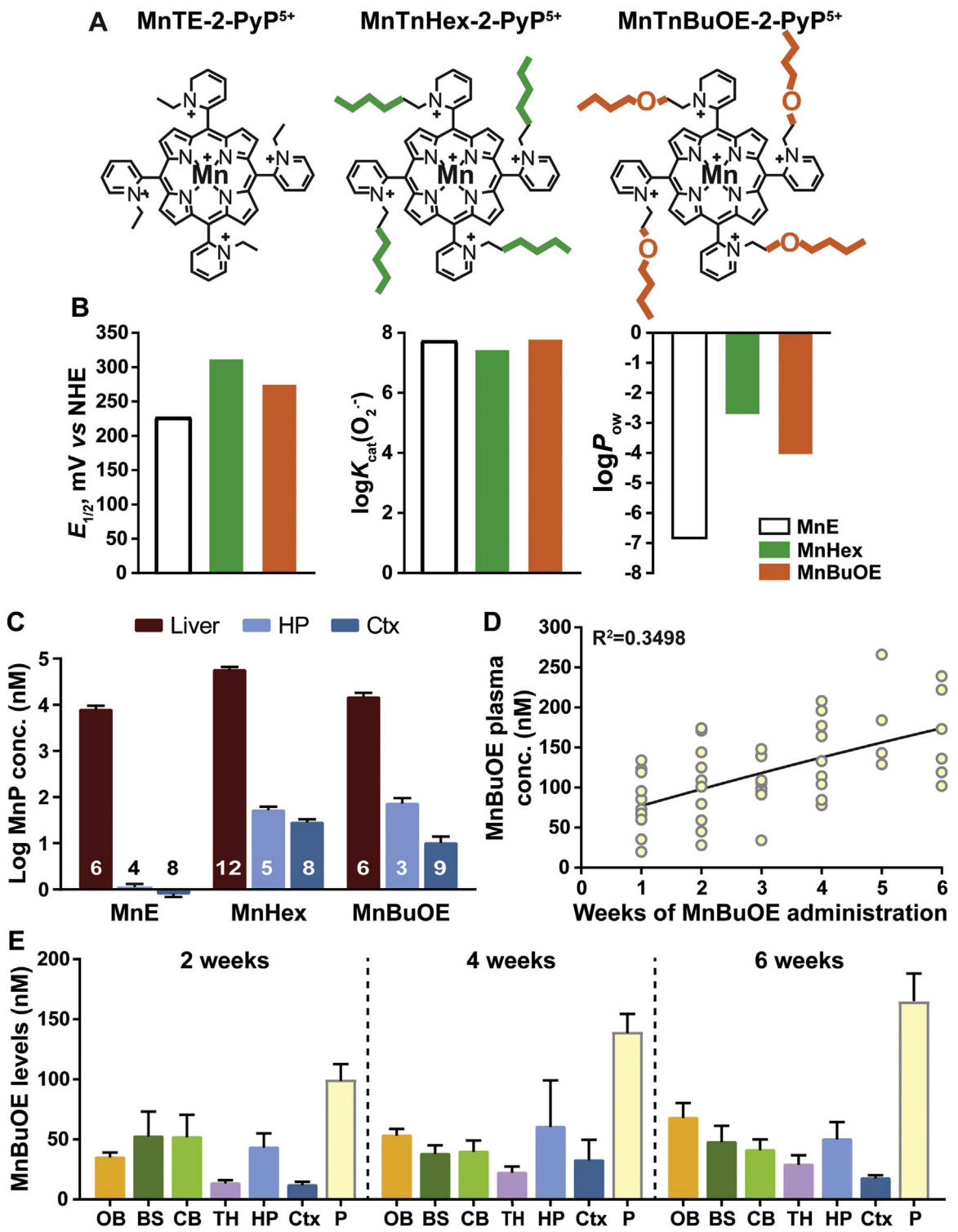

Fig. 1. Structures and tissue levels of Mn porphyrins (MnPs). A, chemical structures of the three MnPs used in this study. **B,** the redox properties of Mn porphyrins expressed in terms of metal-centered reduction potential of $Mn^{III}P/Mn^{II}P$ redox couple, $E_{1/2}$, (in mV vs NHE) (left panel), the rate constant for the catalysis of $O_2^{\cdot -}$ dismutation expressed in log units (middle panel), and the lipophilicity, which controls bioavailability, expressed in terms of the Mn porphyrin distribution between n-octanol and water (right panel). Data are taken from [18]. **C,** MnP levels in the liver, hippocampus, and cortex following a 10-day sc administration of 1.5 mg/kg × 2 per day. Liver values were measured from individual mice; hippocampal values were measured from samples pooled from 2 to 3 mice each; cortical values for MnBuOE and MnE were measured from individual mice; cortical values for MnHex were measured from samples pooled from 2 mice each. Sample sizes are indicated on the bar graph. **D,** cumulative plasma MnBuOE levels from a 6-week administration (3 mg/kg/day via pump with a loading dose of 1.5 mg/kg × 2 via sc injection on day 1). Submandibular bleeding was used for weekly blood collection. Plasma samples collected from individual mice were analyzed. Second order polynomial line fit: $X = 51.01 + 24.81*X + (-0.42)*X^2$. Samples sizes from week 1 to week 6 are: 12, 12, 9, 9, 6, and 6. **E,** MnBuOE levels in various brain regions after 2, 4, or 6 weeks of continuous administration by osmotic pumps. Plasma levels from these three time points were plotted for side-by-side comparisons. Tissues from individual mice were analyzed. Sample sizes for each brain region were 3, 3 and 6 for the 2-, 4- and 6-week measurements, respectively. OB, olfactory bulb; BS, brainstem; CB, cerebellum; TH, thalamus; HP, hippocampus; Ctx, cortex; P, plasma.

oxidizing ascorbate, and oxidizing simple and protein thiols [12]. The thermodynamic and kinetic factors that control SOD-like activity of the Mn porphyrin center also control other redox reactions such as ONOO– reduction, H_2O_2 dismutation and reduction, and ·NO oxidation [13–19].

The radioprotective effects of MnPs have been demonstrated in several cellular and animal models, and most recently in normal brains, salivary glands, and mouth mucosa [20,21]. Moreover, *in vitro* and *in vivo* studies showed differential effects of MnPs on cancer and normal tissues that implied radio- and chemosensitization of cancer tissues and protection of normal tissues [11,20–24]. In this study we first examined three MnPs to identify the best drug to be tested for radioprotection of hippocampal neurogenesis. Based on the biodistribution data in the brain and the lack of overt toxicity, MnBuOE was chosen for follow-up studies.

2. Materials and methods

2.1. Animal studies

Male and female C57BL/6J mice (Jackson Laboratory) were used for various studies starting at 2 months of age. Mice were housed in a pathogen-free facility under standard housing conditions. All animal protocols were reviewed and approved by the IACUC committee at the VA Palo Alto Health Care System and were consistent with the Public Health Service Policy on Humane Care and Use of Laboratory Animals.

2.2. MnP administration

Three MnPs were tested in this study: MnE (Mn(III) *meso*-tetrakis(*N*-ethylpyridinium-2-yl)porphyrin, MnTE-2-PyP^{5+}, BMX-010), MnHex (Mn(III) *meso*-tetrakis(*N*-n-hexylpyridinium-2-yl)porphyrin, MnTnHex-2-PyP^{5+}), and MnBuOE (Mn(III) *meso*-tetrakis(*N*-n-butoxyethylpyridinium-2-yl)porphyrin, MnTnBuOE-2-PyP^{5+}, BMX-001). Based on previous pharmacokinetics, toxicology, and efficacy studies [11,13,20,21,24,25], a daily dose of 3 mg/kg of each MnP was used. Mice received either two daily subcutaneous (sc) injections (2 × 1.5 mg/kg) for 7–14 days, or continuous infusion for 2–6 weeks using a model 1004 Alzet® osmotic pump loaded with 28.4 mg/ml MnP. The concentration was calculated to maintain a total daily dose of 3 mg/kg in a 25 g mouse, which was the average weight of male C57BL/6J mice at 2 months of age. All MnP solutions were diluted in PBS and sterilized with 0.22 μm filters before use.

2.3. Tissue preparation and LC-MS/MS analyses of MnPs

Samples were prepared and analyzed as described [25] with modifications to accommodate small tissue sizes and enhance detection sensitivity. Detailed procedures are described in Supplementary Data.

2.4. Hippocampal neurogenesis studies

Only male mice and MnBuOE were used for neurogenesis studies. The dosing schedules are as depicted in experimental timelines in Figs. 2 and S3. Irradiated mice received a single dose of 5 Gy cranial irradiation using a Mark I gamma irradiator as described [8,26–28]. Immunohistochemical staining and quantification of neuronal populations in the hippocampal dentate gyrus were performed as described [8,26–28].

2.5. Western blot analyses of protein S-glutathionylation

To know if administration of MnBuOE and irradiation led to higher levels of protein *S*-glutathionylation, we treated a separate set of mice with MnBuOE for 7 days followed by a single dose of cranial irradiation. Tissue processing, western blotting, and image analyses were performed as described [8,28,29]. The primary antibodies were anti-glutathione (GSH) (ViroGen, clone D8, 1:2,500) and GAPDH (Sigma, clone GAPDH-71.1, 1:2,500), and a goat anti-mouse IgG tagged with IRDye® 800CW (Li-Cor, 1:10,000) was used as the secondary antibody.

2.6. Statistical analyses

GraphPad Prism 7 was used for statistical analyses. Student's *t*-test was used for simple pair-wise comparisons; one- or two-way analysis of variance (ANOVA) followed by Holm-Sidak's multiple comparisons test was used for comparisons across multiple cohorts. All data are reported as mean ± SEM. Sample sizes are specified in the figure legends.

3. Results

3.1. Tissue levels of Mn porphyrins

We tested three different MnPs – MnE, MnHex, and MnBuOE (Fig. 1A and B) – for their tissue distributions in a 10-day injection study. Acute toxicities from MnHex were observed in 2 mice after 6 days of administration; all other mice appeared to be healthy and their body weights were maintained at a steady level (Fig. S1A). LC-MS/MS analyses showed micromolar concentration of MnPs in the liver, with MnHex showing the highest level, followed by MnBuOE and MnE (Fig. 1C). Consistent with the chemical structure (i.e. increased lipophilicity) that allows MnBuOE and MnHex to cross the blood brain barrier, nanomolar concentrations of MnBuOE and MnHex were detected in various brain regions while only trace amounts of MnE were detected (Figs. 1C and S1B–D). Both MnBuOE and MnHex accumulated at significantly higher levels in the hippocampus than in the cortex (Fig. 1C), with MnBuOE showing a 6-fold difference between the two regions. Because of the observed MnHex acute toxicity, and the potential for long-term toxicity, MnBuOE was chosen for the efficacy studies of radiation protection of hippocampal neurogenesis.

The biodistribution of MnBuOE and MnHex was further tested in a 6-week continuous infusion study. Whereas the plasma showed a steady increase of both MnPs during the 6-week period (Figs. 1D and S2A), brain levels plateaued and did not show significant changes over 6 weeks of infusion (Figs. 1E and S2B). The average hippocampal MnBuOE levels were about 50% of that detected in the 10-day injection study and were 2.4-fold higher than the cortical levels. In contrast, the hippocampal MnHex levels were comparable to that of the 10-day sc injection study. Consistent with the higher toxicity noted above, two out of 9 mice treated with MnHex died around 4 weeks of MnHex administration.

3.2. Hippocampal neurogenesis

The first study was conducted with mice receiving sc injections of MnBuOE one day prior to or one day after irradiation for a total of 7 days (Fig. 2A). No radiation protection was observed with either dosing schedule, and the number of immature neurons (neurons stained positive for the doublecortin (Dcx) protein) was significantly reduced in all irradiated cohorts (Fig. 2C, left panel). The data, combined with known pharmacokinetics of MnBuOE, suggested that longer duration of administration to reach a higher MnBuOE tissue level before irradiation may be necessary to provide effective radiation protection.

Accordingly, one week treatment with MnBuOE before irradiation (Fig. 2B) showed a positive effect in radiation protection of hippocampal neurogenesis (Fig. 2C–F). Consistent with previous study results from EC-SOD transgenic mice [8], higher tissue levels of MnBuOE did not protect Dcx+ neurons from the acute effects of radiation damage when Dcx+ neurons were examined at 48 h after irradiation.

However, at 4 weeks after irradiation, MnBuOE-treated mice produced 31.4% more Dcx+ neurons than the vehicle-treated controls (Fig. 2C, right panel). Detailed analyses revealed that the higher number of Dcx+ neurons seen in the MnBuOE-treated mice was due

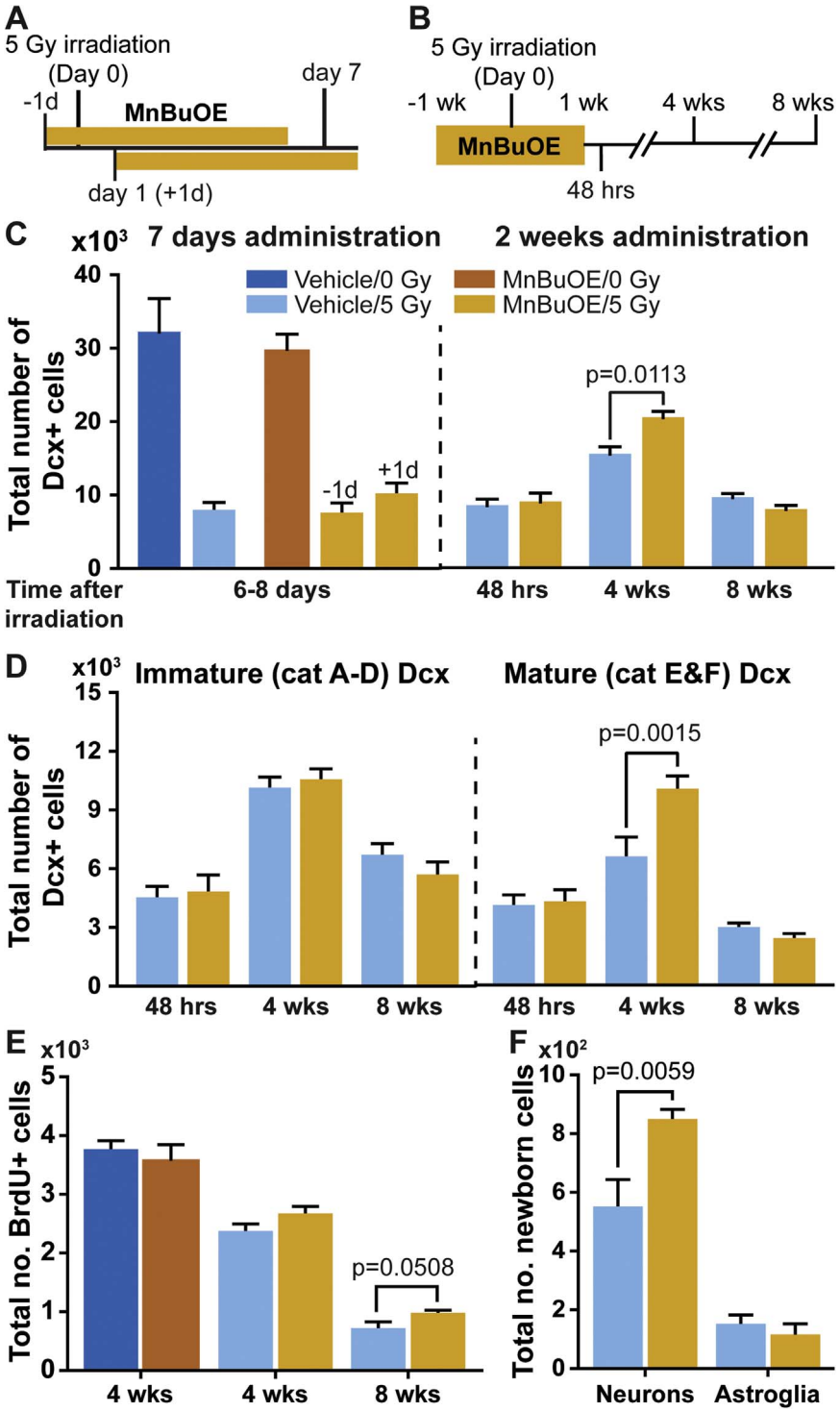

Fig. 2. Efficacy of MnBuOE in radiation protection of hippocampal neurogenesis. Stereological cell counting was used for determining total number of Dcx positive (Dcx+) neurons, BrdU positive (BrdU+) cells, and the production of newborn neurons (BrdU+/NeuN+) and newborn astroglia (BrdU+/GFAP+) in the hippocampal dentate gyrus. **A** and **B,** experimental timelines for the 7-day and 2-week MnBuOE administration, respectively. The day of cranial irradiation was designated as Day 0, and the time points for tissue collections for downstream analyses were indicated. **C,** total number of Dcx+ neurons in the hippocampal dentate gyrus. The intervals between irradiation and tissue collection were indicated in the x-axes. In the 7-day administration study, tissues were collected 6 or 8 days after irradiation from mice that started MnBuOE administration one day before or one day after cranial irradiation, respectively. All the other three cohorts (vehicle/0 Gy, vehicle/5 Gy, and MnBuOE/0 Gy) were sacrificed for tissue collection on day 7. **D,** total number of immature (left panel) and mature (right panel) Dcx+ neurons in the cohorts from the 2-week MnBuOE administration study. **E,** total number of BrdU positive cells in the subgranular zone of hippocampal dentate gyrus at 4 or 8 weeks after cranial irradiation. **F,** lineage analysis of BrdU positive cells in the 8-week cohorts for the production of newborn neurons (BrdU+/NeuN+) and astroglia (BrdU+/GFAP+). One-way ANOVA (C and D) and two-way ANOVA (E and F) followed by Holm-Sidak's multiple comparisons test. Adjusted p values are reported. Sample size: n=4 each in the 7-day injection study; n=5 each in the 2-week injection study.

to the presence of 51.7% more categories E & F Dcx+ neurons, which were neurons with more extensive dendritic arbors [30] (Fig. 2D, right panel). Despite the significant increase in Dcx+ neurons, the extent of progenitor cell proliferation was not improved, and the number of BrdU+ cells in the subgranular zone of hippocampal dentate gyrus was similar between the vehicle- and MnBuOE-treated mice at this time point (Fig. 2E).

At 8 weeks after cranial irradiation, the number of Dcx+ neurons in the hippocampal dentate gyrus were comparable between the vehicle- and MnBuOE-treated cohorts (Fig. 2C and D). However, a modest but significant increase in BrdU+ cells was observed (Fig. 2E), suggesting an enhanced long-term survival of newborn cells from MnBuOE administration. Cell lineage analysis of BrdU+ cells showed a significantly higher number of newborn neurons (BrdU+/NeuN+ cells) in MnBuOE-treated mice, whereas the number of newborn astroglia (BrdU+/GFAP+ cells) were comparable between the two cohorts (Fig. 2F). The data suggested that MnBuOE treatment starting one week prior to and continued for another week after cranial irradiation supported long-term survival of newborn neurons.

Interestingly, prolonged administration of MnBuOE for 6 weeks did not gain additional improvement in hippocampal neurogenesis after cranial irradiation (Fig. S3), and the number of Dcx+ and BrdU+ cells were similar between vehicle- and MnBuOE-treated cohorts (Figs. S3B-C). However, within the Dcx+ population, there was a 23% reduction in the categories A-D and a 57% increase in categories E & F Dcx+ neurons (Fig. S3B).

3.3. Protein S-glutathionylation

In the cortex, MnBuOE and irradiation both contributed significantly to increases in protein *S*-glutathionylation (Fig. 3A), and the level in irradiated/MnBuOE-treated mice showed a significant increase from that of the irradiated/vehicle-treated controls. In contrast, hippocampus from the same experimental animals showed similar levels of protein *S*-glutathionylation across the various treatment groups (Fig. 3B). The hippocampal response (or the lack thereof) was similar to that observed in the liver (Fig. 3C) which was protected from the radiation source during the irradiation procedure.

4. Discussion

In this study we showed that lipophilicity of MnPs dictated their brain distribution, and that MnP levels in the brain did not change during 6 weeks of continuous administration even though the plasma level gradually increased over the same treatment period. We also showed the efficacy of MnBuOE in radiation protection of normal hippocampal neurogenesis when the experimental animals received daily MnBuOE administration for one week prior to and one week after irradiation. Interestingly, extending administration of MnBuOE to 6 weeks did not improve post-radiation hippocampal neurogenesis beyond what was achievable from the two-week administration. Given that MnBuOE is now in clinical trial as a radioprotector of normal brain tissues in glioma patients (trial NCT02655601), this study result has particular clinical relevance.

The SOD-like activities of MnE, MnHex and MnBuOE were determined with cytochrome *c* assay, which was previously shown to give rise to identical data as pulse radiolysis study [31], and were calculated to be 17-, 33- and 15- fold lower, respectively than that of SOD enzymes [18]. However, differences in lipophilicity and structural characteristics dictated their bioavailability in different tissues [13,25,32–34]. Except for the octyl analog, MnHex bioavailability is the highest among the MnPs examined to date [16,25,35,36]. Consistent with those findings, MnHex levels were higher than MnBuOE in most brain regions examined (Figs. 1, S1 and S2). The higher bioavailability of MnHex likely contributes to its higher toxicity in experimental animals seen in this and previous studies [18,37]. On the other hand, the high bioavailability also makes the efficacious doses of MnHex as low as 0.05 mg/kg (see below).

Extensive toxicity studies were done on all three compounds [11,18,25,38,39], and data from more recent studies suggested that none were toxic at the efficacious dose [25,40–42]. While efficacious at the very low dose of 0.05 mg/kg, MnHex had the median toxic dose

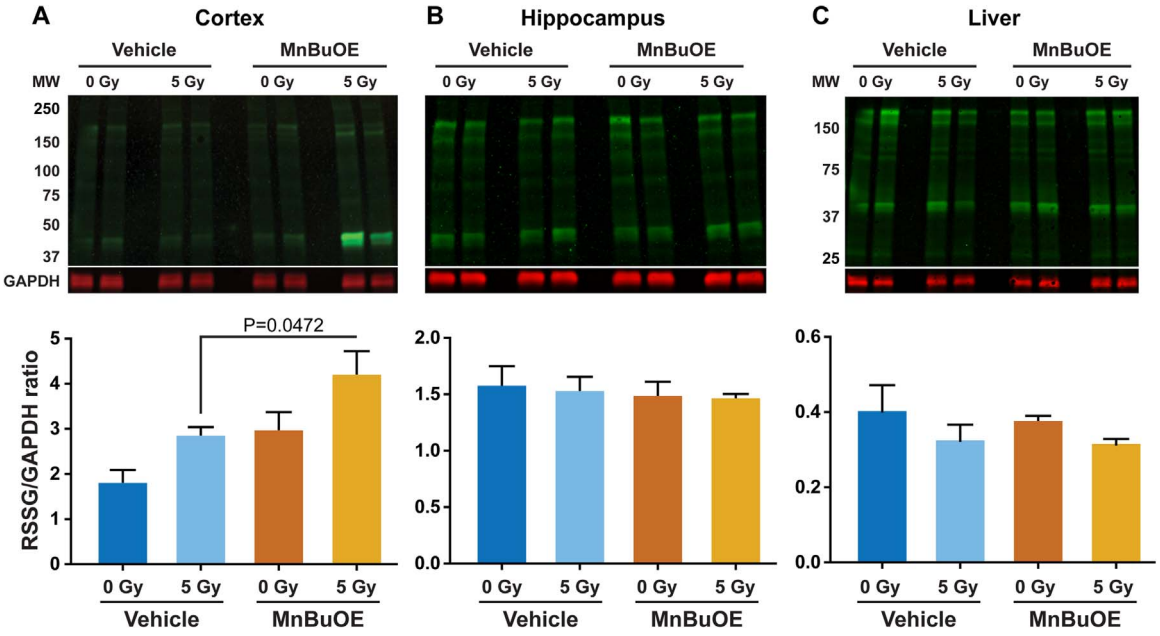

Fig. 3. Protein *S*-glutathionylation. The level of protein *S*-glutathionylation was determined following 7 days of MnBuOE administration (1.5 mg/kg × 2 per day, sc) and/or a single dose of 5 Gy cranial irradiation. Cranial irradiation was performed 4–5 h after the final MnBuOE injection, and tissues collected 3 days later. **A,** cortex; **B,** hippocampus; and **C,** liver. Representative images are shown in the upper panels and quantification of total protein *S*-glutathionylation from western blot images are shown in the lower panels. Signal intensities were normalized to that of GAPDH within each sample. Two-way ANOVA followed by Holm-Sidak's multiple comparisons test. In the cortex, MnBuOE and irradiation both contributed significantly to the differences in the level of protein *S*-glutathionylation (two-way ANOVA; MnBuOE, $F_{(1,12)} = 11.62$, $p = 0.0052$; irradiation, $F_{(1,12)} = 9.564$, $p = 0.0093$). Sample size, $n = 4$ each.

(TD_{50}) measured at 12.5 ± 2.8 mg/kg by subcutaneous administration [38]. At such high concentrations, mice develop severe shivers and hypotonia, in part due to a drop in blood pressure, within several seconds of administration [38]. Histopathology performed at the end of a long-term study (0.5 − 2.5 mg/kg × 2 per day × 4 weeks) showed acute degeneration of hippocampal neurons, mild subcutaneous inflammation, degeneration and regeneration of subcutaneous muscles, and pigment accumulation in Kupffer cells ([18] and Batinic-Haberle et al., unpublished data). However, all mice recovered and showed no overt pathological changes after a 4-week washout period ([18] and Batinic-Haberle et al., unpublished data). The amount of MnHex used in this study was 4 folds below the TD_{50}, but within the range that caused histopathological changes during long-term administration. Consistent with the histopathology findings, we observed gross tissue deformation in the small number of mice that died mid-way through the administration period. A recent study showed the radioprotective effects of MnBuOE on salivary glands and mouth mucosa at a maintenance dose as low as 0.1 mg/kg [43] and suggested that MnHex might have been radioprotective of hippocampal neurogenesis at much lower doses than the one we used in this study.

The MnP measurements showed sample-to-sample variations in some brain regions; some differences were also found in MnP concentrations across brain compartments in two separate studies. The variabilities observed may be ascribed to (a) the heterogeneity of MnP in the tissue, (b) small tissue sample size, such as the hippocampi that weighed 10–15 mg each, (c) the low nanomolar range of MnP concentration which was close to the lower limit of quantification of the LC-MS/MS assay, and (d) the different dynamics of MnP distribution/elimination governed by the different administration methods (daily sc injection vs. continuous pump infusion).

The post-radiation neurogenesis pattern in MnBuOE-treated mice was similar to that observed in EC-SOD transgenic mice with increased number of categories E & F Dcx+ neurons at 4 weeks after irradiation and enhanced long-term survival of newborn neurons (Fig. 2), although the efficacy was modest compared to that from EC-SOD transgenes [8]. Categories E & F Dcx+ neurons have more extensive dendritic outgrowth and branching and are thought to be further along in the maturation process [30]. These more matured Dcx+ neurons should have the advantage of developing into fully functional granule cells, and they likely contributed to the higher number of BrdU+/NeuN+ cells in MnBuOE-treated mice.

Given that the 2-week MnBuOE treatment was efficacious in preserving hippocampal neurogenesis following cranial irradiation, it was somewhat surprising that the 6-week treatment failed to perform better (Fig. S3). We switched to osmotic pump infusion for the 6-week study to reduce stress associated with daily injections. The different administration methods may have contributed to different pharmacokinetics in the tissues such that the hippocampal MnBuOE levels delivered by osmotic pump were roughly half of that delivered by daily injections even though the total daily doses remained the same. Given the different levels of biodistribution and treatment durations, it was difficult for a direct comparison of results from these two studies. Nevertheless, the consistent improvement of hippocampal neurogenesis following cranial irradiation in the MnBuOE-treated cohorts in two separate studies lends strong support to using MnBuOE as the mitigating agent for radiation-associated late effects in the CNS.

Recent data strongly suggest that the major *in vivo* action of MnPs may be the pro-oxidative action at the level of protein thiols, rather than direct scavenging of small reactive species (e.g. O_2^-) [23,29,44,45]. Such action depends on the presence of H_2O_2 and GSH, and its magnitude is directly proportional to the levels of H_2O_2, redox-active drugs, and exogenous H_2O_2 generators in the target tissues. Due to its high abundance in tissues and cells, GSH levels in general were not known to be a limiting factor of MnP-mediated protein *S*-glutathionylation unless the production of GSH is specifically blocked [29,46]. Recent proteomic studies suggested NF-κB to be a major target, and Keap1 to a lesser degree, of MnP-driven catalysis of *S*-glutathionylation [45]. We therefore attempted to see the impact of radiation and MnBuOE on protein *S*-glutathionylation. The lack of increase in total protein *S*-glutathionylation in the hippocampus from treatments with MnBuOE and irradiation was unexpected given the increases seen in the cortex (Fig. 3). Differences between the hippocampus and cortex may have contributed to this outcome, and they include the tissue levels of MnBuOE, capacities for H_2O_2 metabolism, their anatomical locations, and the level of reactive species generated by ionizing radiation as it traverses through the tissues. Consequently, it is difficult to interpret the *S*-glutathionylation results without additional studies into the potential changes in the NF-κB and Keap1/Nrf2 signaling pathways and the magnitude of oxidative stress incurred in each brain region.

5. Conclusion

Our previous studies showed MnBuOE to be efficacious in reducing normal tissue injuries and enhancing sensitivity of cancers to radiation and chemotherapies [13,20,21,23,47,48]. This study expands the normal tissue benefits of MnBuOE to post-irradiation hippocampal neurogenesis, and provides a strong translational support for the current clinical trial of using MnBuOE as a radioprotector. Whether the enhanced hippocampal neurogenesis parallels preserved cognitive functions after cranial irradiation will need to be examined in future studies. The different *S*-glutathionylation outcomes between cortex and hippocampus following MnBuOE treatment and irradiation likely signal differential responses to the treatments. The causes and consequences of such differential response will need to be investigated further in order to optimize treatment conditions to provide a balanced overall benefit to the CNS in patients undergoing cranial radiation therapy. Finally, ionizing radiation leads to multifaceted changes in the CNS. In addition to persistent redox imbalance and inflammation, neurotrophic factor productions are also altered [8,49,50]. Consequently, multidisciplinary treatment including redox active drugs and trophic factors administered, as demonstrated recently [28], at different stages of radiation therapy will likely result in the most favorable outcome in reducing normal tissue damage and increasing functional recovery of the CNS.

Acknowledgement

We thank Xinli Guo for the excellent animal care; Vivian Liao, Melody Khosravi, and David Marash-Whitman for assistance in tissue processing, and Dr. Margaret Tome (University of Arizona) for the consultation in protein *S*-glutathionylation analysis. This work was supported by funding from the VA Merit review BX-0024-71 (TTH), seed grant from Palo Alto Veterans Institute for Research (TTH), NIH/NCI Duke Comprehensive Cancer Center Core Grant (5-P30-CA14236-29) (IS), NC Biotechnology Center BIG Award (#2016-BIG-6518) (IBH, IS and AT), BioMimetix JVLLC (IBH, IS, TW and AT) (186103), Department of Radiation Oncology (IBH), and Brazilian CNPq (402976/2012-6, 485443/2012-0, 552500/2011-9, and 307348/2013-0) and CAPES (24001015030P-4) grants (RSS). We also acknowledge supports from the VA Palo Alto Health Care System for the use of resources and facilities.

Appendix A. Supporting information

Supplementary data associated with this article can be found in the online version at http://dx.doi.org/10.1016/j.redox.2017.04.027.

References

[1] D. Greene-Schloesser, M.E. Robbins, A.M. Peiffer, E.G. Shaw, K.T. Wheeler, M.D. Chan, Radiation-induced brain injury: a review, Front. Oncol. 2 (2012) 73.
[2] L. Padovani, N. Andre, L.S. Constine, X. Muracciole, Neurocognitive function after

radiotherapy for paediatric brain tumours, Nat. Rev. Neurol. 8 (10) (2012) 578–588.
[3] M.L. Monje, H. Toda, T.D. Palmer, Inflammatory blockade restores adult hippocampal neurogenesis, Science 302 (5651) (2003) 1760–1765.
[4] E.I. Azzam, J.P. Jay-Gerin, D. Pain, Ionizing radiation-induced metabolic oxidative stress and prolonged cell injury, Cancer Lett. 327 (1–2) (2012) 48–60.
[5] K. Belarbi, T. Jopson, C. Arellano, J.R. Fike, S. Rosi, CCR2 deficiency prevents neuronal dysfunction and cognitive impairments induced by cranial irradiation, Cancer Res. 73 (3) (2013) 1201–1210.
[6] A. Chakraborti, A. Allen, B. Allen, S. Rosi, J.R. Fike, Cranial irradiation alters dendritic spine density and morphology in the hippocampus, PLoS One 7 (7) (2012) e40844.
[7] J. Raber, R. Rola, A. LeFevour, D. Morhardt, J. Curley, S. Mizumatsu, S.R. VandenBerg, J.R. Fike, Radiation-induced cognitive impairments are associated with changes in indicators of hippocampal neurogenesis, Radiat. Res. 162 (1) (2004) 39–47.
[8] Y. Zou, R. Corniola, D. Leu, A. Khan, P. Sahbaie, A. Chakraborti, D.J. Clark, J.R. Fike, T.T. Huang, Extracellular superoxide dismutase is important for hippocampal neurogenesis and preservation of cognitive functions after irradiation, Proc. Natl. Acad. Sci. USA 109 (52) (2012) 21522–21527.
[9] K. Motomura, M. Ogura, A. Natsume, H. Yokoyama, T. Wakabayashi, A free-radical scavenger protects the neural progenitor cells in the dentate subgranular zone of the hippocampus from cell death after X-irradiation, Neurosci. Lett. 485 (1) (2010) 65–70.
[10] V.K. Parihar, B.D. Allen, K.K. Tran, N.N. Chmielewski, B.M. Craver, V. Martirosian, J.M. Morganti, S. Rosi, R. Vlkolinsky, M.M. Acharya, G.A. Nelson, A.R. Allen, C.L. Limoli, Targeted overexpression of mitochondrial catalase prevents radiation-induced cognitive dysfunction, Antioxid. Redox Signal. 22 (1) (2015) 78–91.
[11] I. Batinic-Haberle, A. Tovmasyan, E.R. Roberts, Z. Vujaskovic, K.W. Leong, I. Spasojevic, SOD therapeutics: latest insights into their structure-activity relationships and impact on the cellular redox-based signaling pathways, Antioxid. Redox Signal. 20 (15) (2014) 2372–2415.
[12] I. Batinic-Haberle, Z. Rajic, A. Tovmasyan, J.S. Reboucas, X. Ye, K.W. Leong, M.W. Dewhirst, Z. Vujaskovic, L. Benov, I. Spasojevic, Diverse functions of cationic Mn(III) N-substituted pyridylporphyrins, recognized as SOD mimics, Free Radic. Biol. Med. 51 (5) (2011) 1035–1053.
[13] A. Tovmasyan, R.S. Sampaio, M.K. Boss, J.C. Bueno-Janice, B.H. Bader, M. Thomas, J.S. Reboucas, M. Orr, J.D. Chandler, Y.M. Go, D.P. Jones, T.N. Venkatraman, S. Haberle, N. Kyui, C.D. Lascola, M.W. Dewhirst, I. Spasojevic, L. Benov, I. Batinic-Haberle, Anticancer therapeutic potential of Mn porphyrin/ascorbate system, Free Radic. Biol. Med. 89 (2015) 1231–1247.
[14] A. Tovmasyan, C.G. Maia, T. Weitner, S. Carballal, R.S. Sampaio, D. Lieb, R. Ghazaryan, I. Ivanovic-Burmazovic, G. Ferrer-Sueta, R. Radi, J.S. Reboucas, I. Spasojevic, L. Benov, I. Batinic-Haberle, A comprehensive evaluation of catalase-like activity of different classes of redox-active therapeutics, Free Radic. Biol. Med. 86 (2015) 308–321.
[15] I. Batinic-Haberle, A. Tovmasyan, I. Spasojevic, An educational overview of the chemistry, biochemistry and therapeutic aspects of Mn porphyrins–From superoxide dismutation to H_2O_2-driven pathways, Redox Biol. 5 (2015) 43–65.
[16] I. Batinic-Haberle, A. Tovmasyan, I. Spasojevic, Mn porphyrin-based redox-active therapeutics, in: I. Batinic-Haberle, J.S. Reboucas, I. Spasojevic (Eds.), Redox-Active Therapeutics, Springer International Publisher, Switzerland, 2016, pp. 165–212.
[17] A. Tovmasyan, S. Carballal, R. Ghazaryan, L. Melikyan, T. Weitner, C.G. Maia, J.S. Reboucas, R. Radi, I. Spasojevic, L. Benov, I. Batinic-Haberle, Rational design of superoxide dismutase (SOD) mimics: the evaluation of the therapeutic potential of new cationic Mn porphyrins with linear and cyclic substituents, Inorg. Chem. 53 (21) (2014) 11467–11483.
[18] A. Tovmasyan, H. Sheng, T. Weitner, A. Arulpragasam, M. Lu, D.S. Warner, Z. Vujaskovic, I. Spasojevic, I. Batinic-Haberle, Design, mechanism of action, bioavailibility and therapeutic effects of Mn porphyrin-based redox modulators, Med. Princ. Pract. 22 (2) (2013) 103–130.
[19] I. Spasojevic, I. Batinic-Haberle, I. Fridovich, Nitrosylation of manganese(II) tetrakis (N-ethylpyridinium-2-yl)porphyrin: a simple and sensitive spectrophotometric assay for nitric oxide, Nitric Oxide: Biol. Chem. 4 (5) (2000) 526–533.
[20] D.H. Weitzel, A. Tovmasyan, K.A. Ashcraft, A. Boico, S.R. Birer, K. Roy Choudhury, J. Herndon 2nd, R.M. Rodriguiz, W.C. Wetsel, K.B. Peters, I. Spasojevic, I. Batinic-Haberle, M.W. Dewhirst, Neurobehavioral radiation mitigation to standard brain cancer therapy regimens by Mn(III) n-butoxyethylpyridylporphyrin-based redox modifier, Environ. Mol. Mutagen 57 (5) (2016) 372–381.
[21] D.H. Weitzel, A. Tovmasyan, K.A. Ashcraft, Z. Rajic, T. Weitner, C. Liu, W. Li, A.F. Buckley, M.R. Prasad, K.H. Young, R.M. Rodriguiz, W.C. Wetsel, K.B. Peters, I. Spasojevic, J.E. Herndon 2nd, I. Batinic-Haberle, M.W. Dewhirst, Radioprotection of the brain white matter by Mn(III) n-Butoxyethylpyridylporphyrin-based superoxide dismutase mimic MnTnBuOE-2-PyP^{5+}, Mol. Cancer Ther. 14 (1) (2015) 70–79.
[22] Y. Yulyana, A. Tovmasyan, I.A. Ho, K.C. Sia, J.P. Newman, W.H. Ng, C.M. Guo, K.M. Hui, I. Batinic-Haberle, P.Y. Lam, Redox-active Mn porphyrin-based potent SOD mimic, MnTnBuOE-2-PyP(5+), enhances carbenoxolone-mediated TRAIL-induced apoptosis in glioblastoma multiforme, Stem Cell Rev. 12 (1) (2016) 140–155.
[23] M.C. Jaramillo, M.M. Briehl, I. Batinic-Haberle, M.E. Tome, Manganese (III) meso-tetrakis N-ethylpyridinium-2-yl porphyrin acts as a pro-oxidant to inhibit electron transport chain proteins, modulate bioenergetics, and enhance the response to chemotherapy in lymphoma cells, Free Radic. Biol. Med. 83 (2015) 89–100.
[24] K.A. Ashcraft, M.K. Boss, A. Tovmasyan, K. Roy Choudhury, A.N. Fontanella, K.H. Young, G.M. Palmer, S.R. Birer, C.D. Landon, W. Park, S.K. Das, T. Weitner, H. Sheng, D.S. Warner, D.M. Brizel, I. Spasojevic, I. Batinic-Haberle, M.W. Dewhirst, Novel manganese-porphyrin superoxide dismutase-mimetic widens the therapeutic margin in a preclinical head and neck cancer model, Int. J. Radiat. Oncol. Biol. Phys. 93 (4) (2015) 892–900.
[25] T. Weitner, I. Kos, H. Sheng, A. Tovmasyan, J.S. Reboucas, P. Fan, D.S. Warner, Z. Vujaskovic, I. Batinic-Haberle, I. Spasojevic, Comprehensive pharmacokinetic studies and oral bioavailability of two Mn porphyrin-based SOD mimics, MnTE-2-PyP and MnTnHex-2-PyP, Free Radic. Biol. Med. 58C (2013) 73–80.
[26] R. Corniola, Y. Zou, D. Leu, J.R. Fike, T.T. Huang, Paradoxical relationship between Mn superoxide dismutase deficiency and radiation-induced cognitive defects, PLoS One 7 (11) (2012) e49367.
[27] Y. Zou, D. Leu, J. Chui, J.R. Fike, T.T. Huang, Effects of altered levels of extracellular superoxide dismutase and irradiation on hippocampal neurogenesis in female mice, Int. J. Radiat. Oncol.*Biol.*Phys. 87 (2013) 777–784.
[28] P. Yang, D. Leu, K. Ye, C. Srinivasan, J.R. Fike, T.T. Huang, Cognitive impairments following cranial irradiation can be mitigated by treatment with a tropomyosin receptor kinase B agonist, Exp. Neurol. 279 (2016) 178–186.
[29] M.C. Jaramillo, M.M. Briehl, J.D. Crapo, I. Batinic-Haberle, M.E. Tome, Manganese porphyrin, MnTE-2-PyP^{5+}, Acts as a pro-oxidant to potentiate glucocorticoid-induced apoptosis in lymphoma cells, Free Radic. Biol. Med. 52 (8) (2012) 1272–1284.
[30] T. Plumpe, D. Ehninger, B. Steiner, F. Klempin, S. Jessberger, M. Brandt, B. Romer, G.R. Rodriguez, G. Kronenberg, G. Kempermann, Variability of doublecortin-associated dendrite maturation in adult hippocampal neurogenesis is independent of the regulation of precursor cell proliferation, BMC Neurosci. 7 (2006) 77.
[31] I. Spasojevic, R. Menzeleev, P.S. White, I. Fridovich, Rotational isomers of N-alkylpyridylporphyrins and their metal complexes. HPLC separation, (1)H NMR and X-ray structural characterization, electrochemistry, and catalysis of O(2)(.-) disproportionation, Inorg. Chem. 41 (22) (2002) 5874–5881.
[32] A. Tovmasyan, J.C. Bueno-Janice, J.S. Reboucas, I. Spasojevic, I. Batinic-Haberle, Redox-active Mn porphyrins, MnTE-2-PyP^{5+} and MnTnBuOE-2-PyP^{5+}, but not redox-inert MnTBAP^{3-}, suppress tumor growth in an environment where H_2O_2 is produced, Free Radic. Biol. Med. 100 (Suppl 1) (2016) S93.
[33] A.M. Li, J. Martins, A. Tovmasyan, J.S. Valentine, I. Batinic-Haberle, I. Spasojevic, E.B. Gralla, Differential localization and potency of manganese porphyrin superoxide dismutase-mimicking compounds in Saccharomyces cerevisiae, Redox Biol. 3 (2014) 1–6.
[34] F.S. Archibald, I. Fridovich, The scavenging of superoxide radical by manganous complexes: in vitro, Arch. Biochem. Biophys. 214 (2) (1982) 452–463.
[35] A. Okado-Matsumoto, I. Batinic-Haberle, I. Fridovich, Complementation of SOD-deficient *Escherichia coli* by manganese porphyrin mimics of superoxide dismutase activity, Free Radic. Biol. Med. 37 (3) (2004) 401–410.
[36] I. Kos, L. Benov, I. Spasojevic, J.S. Reboucas, I. Batinic-Haberle, High lipophilicity of meta Mn(III) N-alkylpyridylporphyrin-based superoxide dismutase mimics compensates for their lower antioxidant potency and makes them as effective as ortho analogues in protecting superoxide dismutase-deficient *Escherichia coli*, J. Med. Chem. 52 (23) (2009) 7868–7872.
[37] Z. Rajic, A. Tovmasyan, I. Spasojevic, H. Sheng, M. Lu, A.M. Li, E.B. Gralla, D.S. Warner, L. Benov, I. Batinic-Haberle, A new SOD mimic, Mn(III) ortho N-butoxyethylpyridylporphyrin, combines superb potency and lipophilicity with low toxicity, Free Radic. Biol. Med. 52 (9) (2012) 1828–1834.
[38] J.M. Pollard, J.S. Reboucas, A. Durazo, I. Kos, F. Fike, M. Panni, E.B. Gralla, J.S. Valentine, I. Batinic-Haberle, R.A. Gatti, Radioprotective effects of manganese-containing superoxide dismutase mimics on ataxia-telangiectasia cells, Free Radic. Biol. Med. 47 (3) (2009) 250–260.
[39] I. Batinic-Haberle, J.S. Reboucas, I. Spasojevic, Superoxide dismutase mimics: chemistry, pharmacology, and therapeutic potential, Antioxid. Redox Signal. 13 (6) (2010) 877–918.
[40] B. Gauter-Fleckenstein, J.S. Reboucas, K. Fleckenstein, A. Tovmasyan, K. Owzar, C. Jiang, I. Batinic-Haberle, Z. Vujaskovic, Robust rat pulmonary radioprotection by a lipophilic Mn N-alkylpyridylporphyrin, MnTnHex-2-PyP(5+), Redox Biol. 2 (2014) 400–410.
[41] S.W. Shin, C. Choi, G.H. Lee, A. Son, S.H. Kim, H.C. Park, I. Batinic-Haberle, W. Park, Mechanism of the antitumor and radiosensitizing effects of a manganese porphyrin, MnHex-2-PyP, Antioxid. Redox Signal. (2017).
[42] H. Saba, I. Batinic-Haberle, S. Munusamy, T. Mitchell, C. Lichti, J. Megyesi, L.A. MacMillan-Crow, Manganese porphyrin reduces renal injury and mitochondrial damage during ischemia/reperfusion, Free Radic. Biol. Med. 42 (10) (2007) 1571–1578.
[43] S.R. Birer, C.-T. Lee, K. Roy Choudhury, K.H. Young, I. Spasojevic, I. Batinic-Haberle, J.D. Crapo, M.W. Dewhirst, K.A. Ashcraft, Inhibition of the continuum of radiation-induced normal tissue injury by a redox-active Mn porphyrin, Radiat. Res. (2017) (in press).
[44] J.C. Bueno-Janice, A. Tovmasyan, I. Batinic-Haberle, Comprehensive study of glutathione peroxidase activity of different classes of redox-active therapeutics - implications for their therapeutic actions, Free Radic. Biol. Med. 87 (2015) S86–S87.
[45] A. Tovmasyan, Y.M. Go, D. Jones, I. Spasojevic, I. Batinic-Haberle, Redox proteomics of 4T1 breast cancer cell after treatment with MnTE-2-PyP5+/ascorbate system, Free Radic. Biol. Med. 100 (Suppl 1) (2016) S112.
[46] D. Pimentel, D.J. Haeussler, R. Matsui, J.R. Burgoyne, R.A. Cohen, M.M. Bachschmid, Regulation of cell physiology and pathology by protein S-glutathionylation: lessons learned from the cardiovascular system, Antioxid. Redox Signal. 16 (6) (2012) 524–542.
[47] R.E. Oberley-Deegan, J.J. Steffan, K.O. Rove, K.M. Pate, M.W. Weaver, I. Spasojevic, B. Frederick, D. Raben, R.B. Meacham, J.D. Crapo, H.K. Koul, The

antioxidant, MnTE-2-PyP, prevents side-effects incurred by prostate cancer irradiation, PLoS One 7 (9) (2012) e44178.
[48] H. Sheng, W. Yang, S. Fukuda, H.M. Tse, W. Paschen, K. Johnson, I. Batinic-Haberle, J.D. Crapo, R.D. Pearlstein, J. Piganelli, D.S. Warner, Long-term neuroprotection from a potent redox-modulating metalloporphyrin in the rat, Free Radic. Biol. Med. 47 (7) (2009) 917–923.
[49] S. Ji, Y. Tian, Y. Lu, R. Sun, J. Ji, L. Zhang, S. Duan, Irradiation-induced hippocampal neurogenesis impairment is associated with epigenetic regulation of bdnf gene transcription, Brain Res. 1577 (2014) 77–88.
[50] Y. Son, M. Yang, S. Kang, S. Lee, J. Kim, J. Kim, S. Park, J.S. Kim, S.K. Jo, U. Jung, T. Shin, S.H. Kim, H. Wang, C. Moon, Cranial irradiation regulates CREB-BDNF signaling and variant BDNF transcript levels in the mouse hippocampus, Neurobiol. Learn. Mem. 121 (2015) 12–19.